

## Tight-Binding Molecular Dynamics of Shock Waves in Methane

J. D. Kress, S. R. Bickham, L. A. Collins, and B. L. Holian

*Theoretical Division, Los Alamos National Laboratory,  
Los Alamos, New Mexico 87545*

S. Goedecker

*Max-Planck Institute for Solid State Research, Stuttgart, Germany  
(Received 26 May 1999)*

The behavior of shock-compressed methane at high temperatures and pressures is studied using nonequilibrium molecular dynamics and linear-scaling tight-binding electronic structure theory in simulations containing as many as 1728 molecules. For certain piston velocities, a chemical dissociation wave evolves that lags behind the compressive shock front. At about 1 ps, the dissociation region consists mainly of molecular hydrogen and hydrocarbon polymers. Shock wave experiments, which access much longer time scales, suggest that the hydrocarbons ultimately decompose into elemental carbon.

PACS numbers: 71.15.Fv, 71.15.Pd, 62.50.+p, 61.20.Ja

Methane is found in many astrophysical environments and is an important constituent of the middle ice layers of the outer gas giants Uranus and Neptune. The pressures and temperatures in this layer range from 20–600 GPa and 2000–8000 K [1] so that understanding the properties of methane under these conditions is critical to the development of accurate planetary models. Determining the transformations induced in hydrocarbons by nonequilibrium phenomena such as shock waves and detonations presents a related problem. The accepted interpretation of shock wave experiments holds that these materials ultimately decompose into elemental carbon (probably amorphous carbon and diamond powder), molecular hydrogen, and perhaps other gases [2,3]. However, recent first-principles molecular dynamics simulations indicate that at pressures above 300 GPa, methane forms a mixture of hydrocarbons [4]. However, the time scale in this study was limited to a few picoseconds, while the carbon residue produced in the shock wave experiments was formed on a much longer time scale. There is clearly a need to determine what transformations occur on an intermediate time scale, as well as to examine the formation of transient species under nonequilibrium conditions.

Analyses of gas-gun shock-compression experiments [3] are based on the Rankine-Hugoniot relations of measured kinematic parameters to thermodynamic variables. The equation of state can then be determined from the pressure-volume ( $P$ - $V$ ) trajectory of the shock adiabat; however, such an approach does not shed light on the dynamical processes in the shock-compressed material. Therefore, in this work we study shock-compressed methane directly with nonequilibrium molecular dynamics (NEMD) using as many as 1728 CH<sub>4</sub> molecules (13 824 valence electrons) and simulation times up to 1.2 ps. We follow the evolution of the fluid as the methane decomposes at high pressures and temperatures into carbon aggregates and molecular hydrogen. We used a recently developed  $O(N)$  tight-binding

(TB) algorithm [5–7] to describe the interatomic forces, where the computational work scales linearly with the number of atoms  $N$ . The valence electrons are treated quantum mechanically via a total-system Hamiltonian constructed from semiempirical matrix elements. The system electronic states are calculated at each MD time step to obtain the interatomic forces. This electronic structure method falls in between classical potentials and *ab initio* methods in terms of accuracy and computational efficiency. The  $O(N)$  algorithm leads naturally to a very efficient parallel implementation; the present calculations have been performed on up to 64 processors on a Silicon Graphics Origin 2000 computer.

We use the Oxford [8–10] TB scheme for hydrocarbons in the simulations, with one  $s$  orbital per hydrogen atom and one  $s$  orbital and three  $p$  orbitals per carbon atom. The scheme is employed self-consistently by enforcing local charge neutrality with a tolerance of  $\pm 0.1$  electronic charge (see Ref. [5] for details). For the pure carbon system, the C-C parameters give reasonable energy versus volume curves for many carbon polytypes, a good description of the phonons and elastic constants for the diamond and graphite structures, and good agreement with *ab initio* calculations for small carbon microclusters. The C-H parameters were fit to give accurate bond lengths and atomization energies for small molecules containing up to five carbon atoms. The original H-H parameters were based on the repulsive interaction between two CH<sub>4</sub> molecules; therefore, the description of a H<sub>2</sub> is only fair (binding energy = 7 eV/molecule and bond length = 0.66 Å). The H-H parameters have been modified [11] to provide better agreement with experiment for H<sub>2</sub> (binding energy = 4.7 eV/molecule and bond length = 0.74 Å) without affecting the description between the H atoms on a given molecule.

All of the simulations employ periodic boundary conditions, whereby a particle exiting the cell through one side

is reintroduced on the opposite side with the same velocity, preserving constant density within the cell. In the equilibrium simulations, an isokinetic ensemble is used, where the temperature is held constant through a simple velocity scaling procedure [12]. With this thermostat, complete equilibrium between translational, rotational, and vibrational degrees of freedom may not occur over the duration of the simulation [13]. For the  $O(N)$  TB algorithm, the kernel polynomial method [5,7] is used with a smeared Fermi function, order 200 Chebyshev polynomials, and a logical truncation of seven hops for the moments.

The nonequilibrium (NE) TB molecular dynamics (MD) simulations of the shock compression employ constant energy dynamics and uniaxial, contracting periodic boundary conditions [14]. The length of the simulation cell in the direction of the compression ( $L_x$ ) decreases in time at a rate proportional to the piston velocity  $u_p$ , whereas the cross-sectional lengths  $L_y$  and  $L_z$  remain fixed. Furthermore, when an atom crosses a boundary ( $y$ - $z$  plane) at either end of the simulation cell, the piston velocity is added or subtracted (to preserve the sense of compression) to the  $x$  component of the atomic velocity. Time steps of 0.5 and 0.25 fs were used in the equilibrium and nonequilibrium simulations, respectively. The shock velocity can be computed directly from the NEMD simulations as the speed of the shock front, where the shock front is determined from the average velocity and density of the particles in equally spaced bins within the supercell [15]. The shock velocity can also be calculated from the initial and final volumes using the Rankine-Hugoniot relation,  $V = V_0[1 - (u_p/u_s)]$ , where  $V_0$  is the initial volume,  $u_s$  is the velocity of the shock wave, and  $u_p$  is the mass (piston) velocity behind the shock front. The density in each bin is more accurately determined than the average particle velocity, since the latter is computed by Eulerian transformation. Therefore, generally we utilize the  $u_s$  derived from the compression ratio,  $V_0/V$ , although, in the present work, both methods give consistent results. Once  $u_s$  is determined, the shock pressure is computed from  $P - P_0 = \rho_0 u_s u_p$ , where the initial pressure  $P_0$  is effectively zero for the single-shock situations and  $\rho_0$  is the initial density.

Equilibrium TBMD simulations were first carried out in a constant-volume cell to study the behavior of  $\text{CH}_4$  at a volume of  $V = 10.04 \text{ cm}^3/\text{mol}$  corresponding to the final second-shock state from a gas-gun experiment [3]. We used a periodic cubic simulation cell of length  $L = 12.88 \text{ \AA}$  containing 54  $\text{CH}_4$  molecules and performed isokinetic simulations at temperatures between  $T = 1000$  and 8000 K. For both the original and modified Oxford TB schemes, there is a change [5] in the slope of pressure versus temperature between 4000 and 5000 K. The structure of the fluid has been characterized by analyzing the pair correlation functions and nearest-neighbor distributions for C-C, C-H, and H-H. For 4000 K and below, the system remains a  $\text{CH}_4$  fluid, but for 5000 K and above, the molecules dissociate. At 5000 K, the molecules begin

to dissociate at 3 ps with the system evolving into a mixture of  $\text{H}_2$  and hydrocarbon polymers after 10 ps. The pressure ( $P = 77 \text{ GPa}$ ) at 5000 K agrees well with a constant-volume *ab initio* molecular dynamics (AIMD) simulation [16] for a 16 molecule supercell ( $P = 81 \text{ GPa}$ ), where the fluid also dissociates. The composition of the mixture from the TBMD simulation at 5000 K is similar to that observed in a constant-pressure AIMD simulation [4] of a 16 molecule at  $P = 100 \text{ GPa}$ .

We next consider single-shock gas-gun experiments [3,17] with an initial state ( $\rho_0 = 0.423 \text{ g/cm}^3$ ,  $V_0 = 37.9 \text{ cm}^3/\text{mol}$ ,  $T = 111 \text{ K}$ ) that was prepared with an equilibrium isokinetic MD simulation for 432  $\text{CH}_4$  molecules corresponding to cell dimensions of  $L_x = 120.3 \text{ \AA}$  and  $L_y = L_z = 15.0 \text{ \AA}$ . NEMD simulations were performed for piston velocities between 2.2 and 8.3 km/s, corresponding to the experimental values. The calculated shock velocity is shown in Fig. 1 along with the measurements from the single-shock experiments [3,17] and the results from statistical-mechanical/chemical-equilibrium calculations [2]. As  $u_p$  increases and the fluid begins to dissociate, experiment and simulation agree due to the accuracy of the *intramolecular* potential for the breaking and making of bonds afforded by the semiempirical description of the electronic structure. A linear fit to the experimental results yields [3] an intercept, the bulk isentropic sound speed  $C = 2.84 \text{ km/s}$ , whereas the NEMD results yield  $C = 0.6 \text{ km/s}$ . The discrepancy in the sound speeds arises from the less accurate description of the long-range *intermolecular* potential between  $\text{CH}_4$  molecules provided by the Oxford TB. However, at high compressions

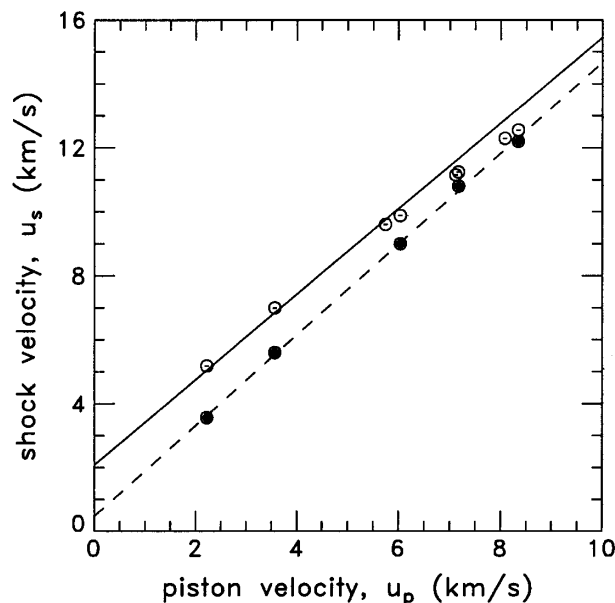


FIG. 1. Shock velocity as a function of piston velocity. Solid circles are NEMD results, while the open circles are from gas-gun experiments [3,17]. The dashed line is a linear fit to the NEMD results, and the solid line was derived using a statistical-mechanical/chemical-equilibrium model [2].

considered in the present work, these weak long-range interactions are less important relative to the intramolecular forces.

Although the average particle velocity and density (pressure) in the compressed region reach steady-state values within a few hundreds of femtoseconds, the temperature and chemical composition of the compressed region do not reach complete equilibrium on a time scale that allows reasonable computational effort. Therefore, to determine the equilibrium chemical composition of the system, additional equilibrium isokinetic MD calculations were performed on 54-molecule simulation cells corresponding to the density and average temperature for each point in Fig. 1. For  $u_p = 7.165$  km/s ( $P = 33$  GPa) or less, the  $\text{CH}_4$  fluid did not dissociate on the time scale of our simulations, but for  $u_p = 8.34$  km/s ( $P = 43$  GPa,  $V = 12.0$  cm<sup>3</sup>) or greater, the  $\text{CH}_4$  fluid decomposed into a mixture of carbon polymers and molecular hydrogen. These results predict dissociation at slightly higher pressures compared to statistical-mechanical/chemical-equilibrium calculations [2], but are consistent with electrical conductivity measurements [17] that indicate no dissociation occurs for a  $u_p = 8.08$  km/s shock ( $P = 42$  GPa). However, this dissociation transition appears sensitive to the models.

Next, we performed a NEMD simulation to mimic a double shock experiment [3] and investigate the chemical dissociation in more detail. We use the experimental first-shock state as an initial state and a piston velocity of  $u_p = 4.06$  km/s, chosen to approximately reproduce the final experimental compression. The resulting state ( $P = 75$  GPa,  $V = 10.45$  cm<sup>3</sup>/mol) has a volume within 5% of experiment and a pressure about 80% of experiment. The configuration for the initial state ( $L_x = 352$  Å) in this simulation consists of 1728 isolated  $\text{CH}_4$  molecules (no bonding between C atoms). The configuration for  $t = 1100$  fs ( $L_x = 260$  Å) from a 4800 time step NEMD shock compression is shown in Fig. 2. (Approximately 200 CPU hours on 64 processors of a Origin 2000 Silicon Graphics computer was used for the simulation.) Relative to the initial state, the shock has compressed the fluid by a factor of 1.4 and induced a chemical reaction, namely, polymerization of the methane into hydrocarbon chains (clusters) containing two or more C atoms. The bonds between C atoms in these clusters are plotted in the upper panel, while all the bonds are shown in the expanded view in the lower panel. The latter illustrates that the system may be viewed as isolated carbon/hydrocarbon polymer islands in a sea of molecular hydrogen (the white-white bonds in Fig. 2).

The left panel of Fig. 3 depicts the density profile of one-half of the simulation cell after propagation of a shock wave produced by a piston velocity of  $u_p = 4.06$  km/s. The shock and piston are both moving from left to right, and time increases along the ordinate. The wedge in the upper left corner of the figure is the "region" vacated

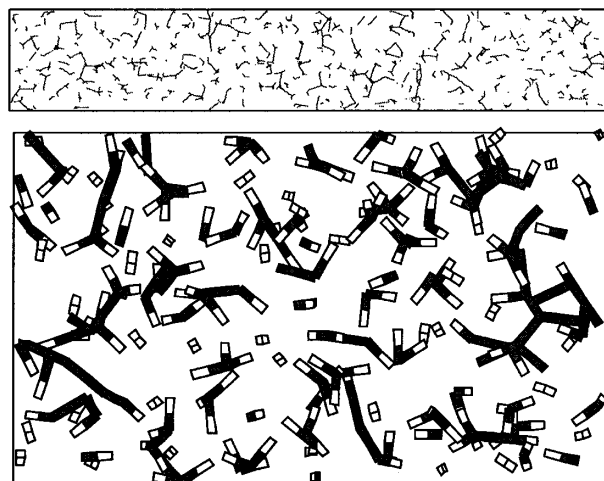


FIG. 2. View of the methane supercell (with one piston face at the right-hand end) after propagation of a shock wave. One-fourth the cell and only bonds between C atoms are shown in the upper panel, while 1/16th of the cell and all bonds are shown in the expanded lower panel. C half-bonds are dark and H half-bonds are white.

upon compression by the piston, while the shock front is visible as a boundary between the compressed orange region and the uncompressed green region. This boundary has a thickness of only a few atomic diameters. The shock front has just reached the center of the simulation cell (position = 0 Å) at  $t = 1.2$  ps. The shock velocity and compression ratio are  $u_s = 14$  km/s and  $\rho/\rho_0 = 1.41$ .

After the shock wave has propagated for approximately 800 fs, a dissociation/association wave is formed in the shocked portion of the sample. The spatial and time dependences of these reactions are characterized using a nearest-neighbor analysis and plotted in the right-hand panel of Fig. 3 for hydrogen. The region vacated upon compression was assigned a value of  $-0.2$  to distinguish it from the unshocked portion of the sample, which contains only methane and, on the average, no H-H nearest neighbors within the cutoff radius of 1.0 Å. Molecular hydrogen corresponds to an average number of one hydrogen nearest neighbor. As the shock wave propagates through the material, the high temperature induces dissociation into H atoms and methyl radicals. Nearly simultaneously, the high pressure and density then promotes the formation of molecular hydrogen and  $\text{C}_2\text{H}_6$  and other polymers. After 1 ps, about half of the H atoms in the shocked portion of the sample have combined to form  $\text{H}_2$ . Analysis of the C-H and C-C nearest-neighbor distributions indicates that each C atom has an average of  $\sim 1$  C and  $\sim 3$  H neighbors at the end of the simulation, compared to initial values of 0 and 4, respectively. The local temperature at  $t = 1.2$  ps, as determined from the transverse components of the kinetic energy, ranges from 15 000 K at the piston face to 9000 K just behind the shock front.

In conclusion, the TBMD simulations presented here demonstrate that shock wave dynamics in methane is more

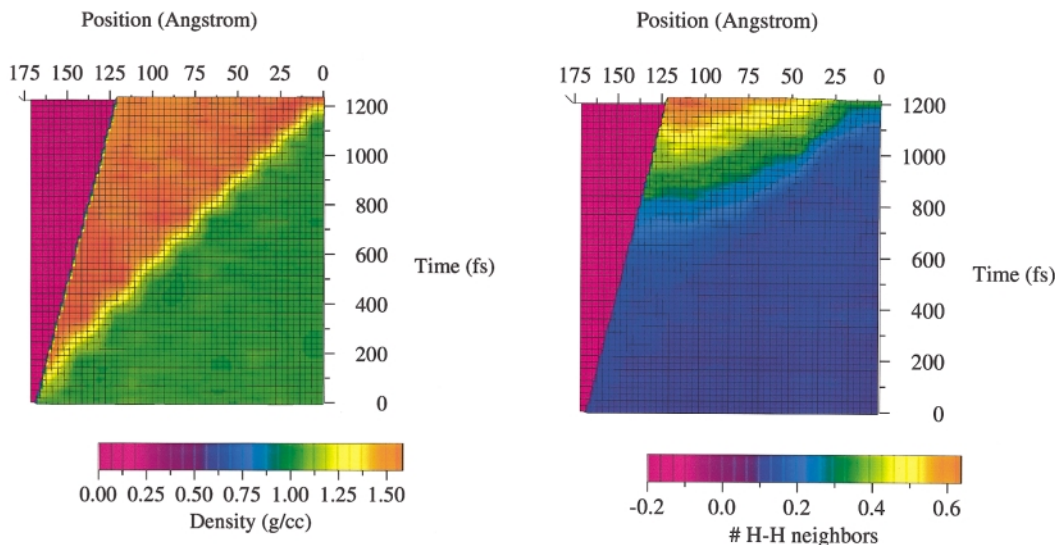


FIG. 3 (color). Propagation of a shock wave in a 352 Å supercell containing 1728 methane molecules. The left panel shows the density profile, while the right panel shows the average number of H neighbors for each H atom.

complex than suggested by a postmortem analysis of experiments. The first 0.8 ps of shock wave propagation is marked by the dissociation of methane into H atoms and methyl radicals. At high pressures and densities these species “cook” and associate into molecular hydrogen and carbon polymers. This dynamic analysis reveals the time scale for experimentally probing these dissociation products and should be valuable for understanding the behavior of hydrocarbon materials during detonations. The quantum mechanical (TB) description for methane provides a good model to study the dynamics of dissociating molecular fluids (making and breaking of chemical bonds) at high temperatures and pressures. Future improvements to the TB description should include improving the accuracy of the van der Waals forces for simulations at low temperatures and pressures.

This work was performed with support from the Advanced Strategic Computing Initiative program under the auspices of the U.S. Department of Energy at Los Alamos National Laboratory (LANL) under Contract No. W-7405-ENG-36. Most of the calculations were performed at the Advanced Computing Laboratory at LANL.

[1] W.B. Hubbard and J.M. MacFarlane, *J. Geophys. Res.* **85**, 225 (1980).

[2] M. Ross and F.H. Ree, *J. Chem. Phys.* **73**, 6146 (1980).

[3] W.J. Nellis, F.H. Ree, M. van Thiel, and A.C. Mitchell, *J. Chem. Phys.* **75**, 3055 (1981).

[4] F. Ancilotto, G.L. Chiarotti, S. Scandolo, and E. Tosatti, *Science* **275**, 1288 (1997).

[5] J.D. Kress, S. Goedecker, A. Hoisie, H. Wasserman, O. Lubeck, L.A. Collins, and B.L. Holian, *J. Comput. Aided Mater. Design* **5**, 295 (1998).

[6] S. Goedecker and L. Colombo, *Phys. Rev. Lett.* **73**, 122 (1994); S. Goedecker, *Rev. Mod. Phys.* **71**, 1085 (1999).

[7] A.F. Voter, J.D. Kress, and R.N. Silver, *Phys. Rev. B* **53**, 12 733 (1996).

[8] A.P. Horsfield, P.D. Godwin, D.G. Pettifor, and A.P. Sutton, *Phys. Rev. B* **54**, 15 773 (1996).

[9] C.H. Xu, C.Z. Wang, C.T. Chan, and K.M. Ho, *J. Phys. Condens. Matter* **4**, 6047 (1992).

[10] B.N. Davidson and W.E. Pickett, *Phys. Rev. B* **49**, 11 253 (1994).

[11] The hopping integral and pair repulsion term has been scaled by 0.682 and the cutoff for each has been changed from 1.22 to 1.50 Å.

[12] M.P. Allen and D.J. Tildesley, *Computer Simulation of Liquids* (Oxford Science, Oxford, 1987).

[13] J.D. Johnson, M.S. Shaw, and B.L. Holian, *J. Chem. Phys.* **80**, 1279 (1984).

[14] B.L. Holian, *Phys. Rev. A* **37**, 2562 (1988).

[15] B.L. Holian, W.G. Hoover, B. Moran, and G.K. Straub, *Phys. Rev. A* **22**, 2798 (1980).

[16] L.A. Collins (unpublished).

[17] H.B. Radousky, A.C. Mitchell, and W.J. Nellis, *J. Chem. Phys.* **93**, 8235 (1990).